AIAA JOURNAL
Vol. 38, No. 2, February 2000

Turbulence Production and Transport in Quasi-Two-Dimensional Wake/Boundary-Layer Interaction

G. A. Sideridis,* E. G. Kastrinakis,† and S. G. Nychas‡
Aristotle University of Thessaloniki, 540 06 Thessaloniki, Greece

The turbulent kinetic energy aspects related to production and transport in the wake of a cylinder interacting with a boundary layer have been investigated experimentally. Using a simple but efficient technique, the velocity power spectral characteristics in the intermediate wake were modified to comply with the requirements for quasi-two-dimensional behavior, i.e., to display a scaling region deviating from the $-\frac{5}{3}$ power law, which is typical of homogeneous, three-dimensional turbulence. The cylinder was placed parallel to the plate and normal to the flow, with its wake developing just outside of the boundary layer but with its lower part in contact and interacting with it. The streamwise and normal-to-the-plate velocity components have been recorded simultaneously in the intermediate wake using hot-wire anemometry. In addition to the calculation of kinetic energy production, third-order correlations of the two velocity fluctuation components, denoting streamwise and lateral transport of the corresponding kinetic energy terms, have also been evaluated. There is significant reduction of kinetic energy production in the lower half wake, in contact with the boundary layer, as compared to the upper half on the freestream side. This is associated with a considerable buildup of kinetic energy production within the boundary-layer flow. The transport mechanisms in the present flow have been investigated and are discussed to provide a basis for formulation and refinement of numerical models and methodologies.

I. Introduction

INTERACTING flows, such as those in the present case of a turbulent wake and a boundary layer, are encountered in many and very diverse engineering applications as well as in environmental flows. Their properties, and especially the associated entrainment and mixing processes, influence directly phenomena such as heating and cooling, chemical reaction development, aerodynamic performance, dispersion of atmospheric pollutants, etc. It has been established that the primary mechanism of entrainment is large-scale engulfment, whereas mixing and diffusion are related to small-scale perturbations.[1,2] The large-scale organized structures present in a turbulent wake play a very important role in both entrainment and mixing, in the sense that these structures are associated with vortex stretching and, therefore, with intense turbulent production.[3] Turbulent kinetic energy is transported away from regions of high turbulence as new fluid from the surrounding flow is entrained. A measure of such a kinetic energy flux is provided by the triple products of the velocity fluctuation terms. Very few works on this subject can be found in the literature, and these refer to the case of a cylinder wake in a free flow.[4] Fabris[5] reported that considerable variations exist among the lateral and streamwise transport intensities of the kinetic energy terms.

In the present experimental work the wake of a circular cylinder formed in a free flow was interacting with a boundary layer developing along a flat plate. The large-scale structures present in the wake, the von Kármán vortices, have received considerable attention from many authors.[6,7] An extensive description of their topological details and properties can be found in a publication by Hussain and Hayakawa,[8] who reported that except for an overall reduction of their strength with streamwise distance the von Kármán vortices retain their well-defined staggered organization, their strong coherent nature, and their distinct periodicity in the intermediate wake ($10 < x/D < 50$, $D =$ cylinder diameter). Rather few experimental studies of the case of a cylinder wake interacting with a boundary layer may be found in the literature. Usually, the cylinder is immersed in the boundary layer at various heights from the surface, and vortex formation characteristics are examined.[9–11] However, numerical simulations of vortex interactions with solid surfaces have been considered much more extensively.[12,13] In numerical studies a single two-dimensional vortex is examined, traveling in a freestream and passing close to a wall, close enough to interact with the boundary layer.[14] It is very difficult to produce such pure flows in the laboratory for validation of numerical methods. Usually, a series of vortices is produced (e.g., a von Kármán street) that have a two-dimensional character, but essentially, they are three dimensional.

By the term two-dimensional it is implied that one fluctuating velocity component is suppressed compared to the others; in the case just mentioned it is the velocity component along the axis of the cylinder generating the vortex street. Another characteristic associated with quasi-two-dimensional turbulence is the existence in the velocity power spectrum of a scaling region following a power law with the exponent deviating from the value $-\frac{5}{3}$, which is typical for isotropic, three-dimensional turbulence. A generally accepted exponent value for quasi-two-dimensional turbulence is of the order of -3. An example of a real flow with such turbulence characteristics is the high-altitude atmospheric flow.[15] In this case quasi-two-dimensional turbulence displays itself by motion planes parallel to the Earth's surface. Air moves primarily along these planes but not in a perpendicular direction to them. An extensive discussion on the differences between two- and three-dimensional turbulent flows is presented in Ref. 16.

To produce in the present study experimental results that can be used for numerical model validation and also for a qualitative investigation of the atmospheric flow, particular attention was given to enhance the two-dimensional characteristics of the present flow. During an earlier work,[17] the observation was made that a cylinder with rough surface produced a wake with velocity power spectra with exponent close to $-\frac{7}{3}$ in a region bounded by the limits $y'/D < \pm 2$, $10 < x/D < 40$, and with a Reynolds number R_D within the range $1500 < R_D < 3000$ (y' is measured from the spanwise plane of symmetry). For that reason a circular cylinder covered with high-grade sandpaper was used for the present experiments. The spanwise velocity component w (i.e., that along the cylinder's longitudinal axis) has not been measured systematically. A few exploratory measurements in the wake at $x/D = 25$ indicated a 30% lower rms value of w relative to the other velocity components. This still significant presence of w implies that there might be important three-dimensional effects present in the flow.

Received 18 May 1998; revision received 15 May 1999; accepted for publication 14 July 1999.

*Postdoctoral Researcher, Department of Chemical Engineering, University Box 453.
†Assistant Professor, Department of Chemical Engineering, University Box 453.
‡Professor, Department of Chemical Engineering, University Box 453.

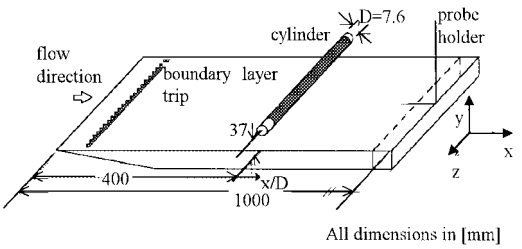

Fig. 1 Sketch of the experimental configuration.

II. Experimental Setup

The present experimental work was contacted in an open-return, suction-type wind tunnel. The dimensions of the test section were $0.3 \times 0.3 \times 2$ m, and the freestream turbulence level there was less than 0.4%. The configuration used is shown in Fig. 1. Special care was given to position the plate in the test section with its top surface parallel to the main flow to avoid flow separation at the sharp leading edge. The boundary layer was tripped near the leading edge to ensure fully turbulent flow development along the plate. A tripping device like the one proposed by Hama[18] was used. It consisted of a row of thin triangular patches pasted on the surface of the plate. A spiral motion is promoted in the space between two neighboring triangles, resulting in consistent three-dimensional vortex shedding, which tripped the boundary layer.

The cylinder with diameter $D = 7.6$ mm was placed at a height above the plate $h_c = 5D$. The local boundary-layer thickness was $\delta_0 \approx 3D$, and consequently $(h_c/\delta_0) \approx 1.6$. The value of h_c was selected such that the wake of the cylinder and the associated von Kármán vortices were formed and developed initially in the free flow, well above the boundary layer, but close enough for interaction to occur at a streamwise distance of about $10D$.

Hot-wire anemometry was used throughout the present measurements. An X-type, double-wire probe (DANTEC 55P61) was employed, operated by a multichannel anemometer system, type AN-1003 of A. A. Lab Systems, Ltd. A low-overheat ratio (30%) was selected to avoid thermal interference between the wires. The probe output signals were digitized by an 8-channel 16-bit analog to digital converter (Data Translation DT-2809), and then they were fed to a personal computer for processing. Sampling frequency was 4 kHz per channel, and 163,000 samples were taken per recording.

The probe recorded simultaneously, at any point, the streamwise and the normal velocity components $U(t) = \bar{U} + u(t)$ and $V(t) = \bar{V} + v(t)$. (An overbar denotes time-averaged values, and lowercase letters denote fluctuations.) The estimated error in the measurement of the velocity components is ±2.5%. Throughout the present experiments the freestream velocity was $U_0 = 3.5$ m/s, giving $R_D = 1820$. The friction velocity U_τ, referred to the plate and obtained from a $[U_0 - U_{(y)}]/U_\tau$ vs y/δ_0 Clauser plot, was $U_\tau = 0.175$ m/s. The turbulence Reynolds numbers R_l and R_λ, based on Kolmogorov's length l estimated to 0.2 mm and Taylor's microscale λ, estimated to 3.4 mm, were evaluated to 50 and 820, respectively. The length l was deduced from the relation: $l = [\nu^3/\varepsilon]^{1/4}$, where $\nu = 1.465 \cdot 10^{-5}$ the kinematic viscosity of air and ε = energy dissipation rate. The latter was evaluated using the isotropic turbulence relation: $\varepsilon_I = 15\nu(\partial u/\partial x)^2$, which simplified to $\varepsilon_I = (15\nu/\bar{U}^2)(\partial u/\partial t)^2$ by invoking Taylor's hypothesis. The term $(\partial u/\partial t)^2$ was deduced from the streamwise velocity fluctuation time series. The length λ was obtained from the relation $\lambda = [u^2/(\partial u/\partial x)^2]^{1/2}$, which also simplified to $\lambda = [u^2 \cdot \bar{U}^2/(\partial u/\partial t)^2]^{1/2}$ using similarly the Taylor's hypothesis.

The probe was traversed from a point well inside the free flow to a distance of 4 mm from the surface of the plate. Four measuring stations have been considered in the streamwise direction at $x/D = 20$, 25, 30, and 35.

III. Results

A. Mean Flow

Profiles of the mean streamwise velocity $\bar{U}/U_0$ across the present interacting flows as well as across the boundary-layer flow alone, without the presence of the wake, are shown in Fig. 2. Normalized velocity is plotted against normalized distance from the plate

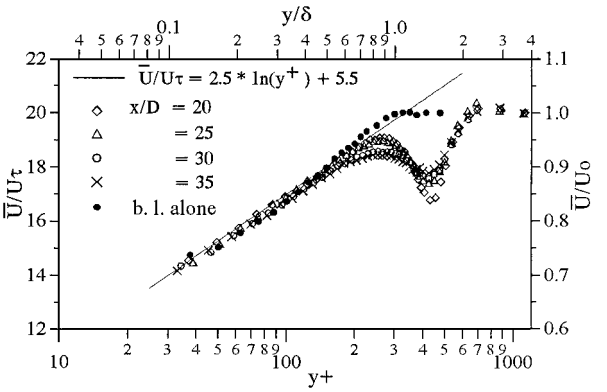

Fig. 2 Logarithmic distribution of the mean streamwise velocity measured across the interacting wake and boundary-layer flows and, also, across the boundary-layer flow in the absence of the wake.

$y^+ (= U_\tau y/\nu)$. A logarithmic scale has been used to compare the velocity profiles to a logarithmic law, typical of fully turbulent flow. As indicated in Fig. 2, the lower part of the velocity profiles ($30 < y^+ < 200$) coincide with the logarithmic law, denoting a fully turbulent boundary-layer flow. The upper part of the profiles ($200 < y^+ < 800$) displays a velocity defect, as expected within the wake of the cylinder. This is defined at every streamwise location as follows: $U_d = U_0 - U_{\min}$ ($U_{\min}$ = minimum velocity in the wake).

B. Velocity Power Spectral Characteristics

Figures 3a and 3b show the normal velocity power spectra at the first and the last measuring station, respectively. In each figure two pairs of curves are shown. The lower pair displays actual velocity spectrum plots at a distance of two diameters on each side of the cylinder's spanwise plane of symmetry ($y'/D = \pm 2$). The upper-half wake curve has been shifted upward by 2.9×10^{-5} for clarity. The upper pair of curves has been produced by multiplication of the ordinates of the actual spectra by f^n, where f is the corresponding values of frequency and n is the anticipated slope of the scaling region; at present, $n = \frac{7}{3}$. The effect of this transformation is that it forces the part of the spectrum, which follows a power law with exponent $-n$, to become horizontal.[19] Horizontal lines have been drawn in each figure to facilitate the determination of the horizontal section of each of the compensated spectral distribution. There is some difficulty involved in this task as the final outcome is primarily a matter of judgement. The results presented in Figs. 3a and 3b, marked by broken lines, are certainly subject to the preceding conditions. However, we do believe that they indicate regions in the velocity power spectra that follow a power law with exponent close to $-\frac{7}{3}$. Steeper turbulence decay rates, close to -4, are present at higher frequencies.

Figure 3a shows that at $x/D = 20$ both velocity spectrum plots display well-defined peaks at the Strouhal frequency (≈100 Hz), indicating the presence of strong von Kármán vortices. Also, both plots have scaling regions with slope close to $-\frac{7}{3}$, extending from about 200 to 600 Hz. Hence, at $x/D = 20$ there are not any great differences between the upper and the lower half wakes, presumably because the interaction with the boundary layer has not been developed considerably yet. Figure 3b shows that at $x/D = 35$ the peak at the Strouhal frequency, although weaker, is still well defined in the upper-half wake. On the contrary, in the lower-half wake, a peak at the Strouhal frequency is merely identifiable. Figure 3b also shows that there is a scaling region in the upper-half wake with slope close to $-\frac{7}{3}$ extending over the same frequency range as in Fig. 3a. In the lower-half wake, however, the corresponding part has been reduced significantly. Hence, it can be argued that the lower-half wake has been affected extensively by the interaction with the boundary layer through a drastic reduction of the strength of the large-scale vortices.

C. Turbulent Kinetic Energy Production and Distribution

The usual turbulent kinetic energy production term $-\overline{uv}(d\bar{U}/dy^+)$ has been evaluated across the wake and the boundary layer at all measuring stations. The $\overline{uv}$ Reynolds-stress component was

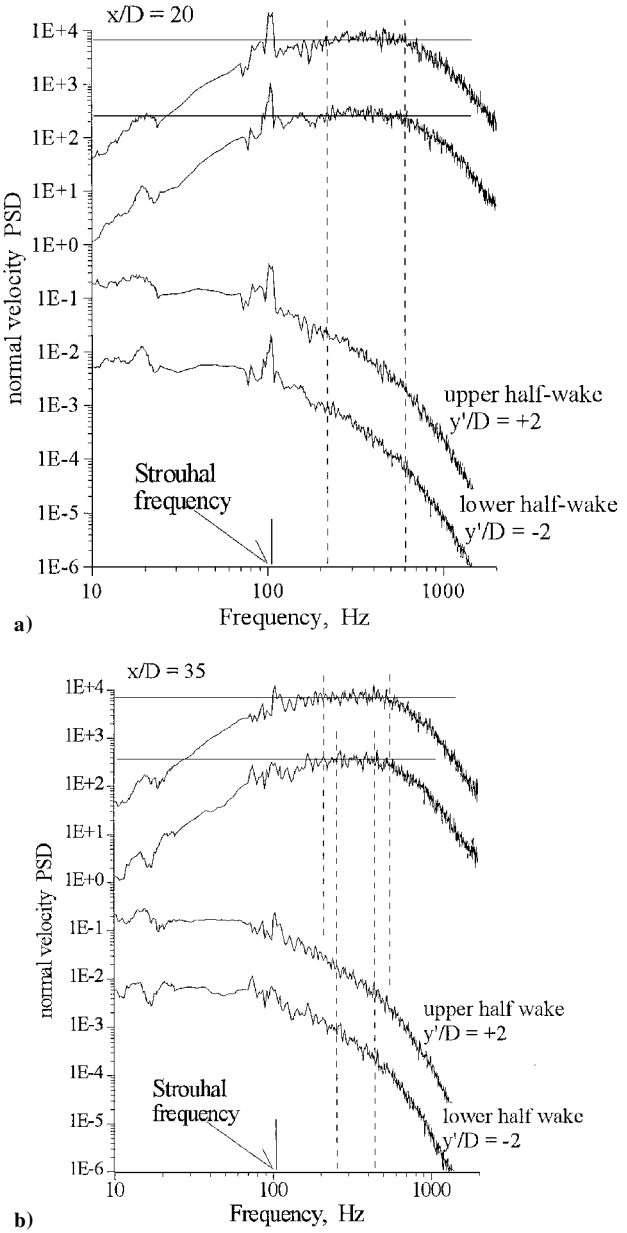

Fig. 3 Normal velocity power spectrum at $y'/D = \pm 2$ and at a) $x/D = 20$ and b) $x/D = 35$ (y' is measured from the wake centerline). Lower pair: actual velocity power spectrum. Upper pair: (ordinate) × (frequency)$^{7/3}$ vs (frequency).

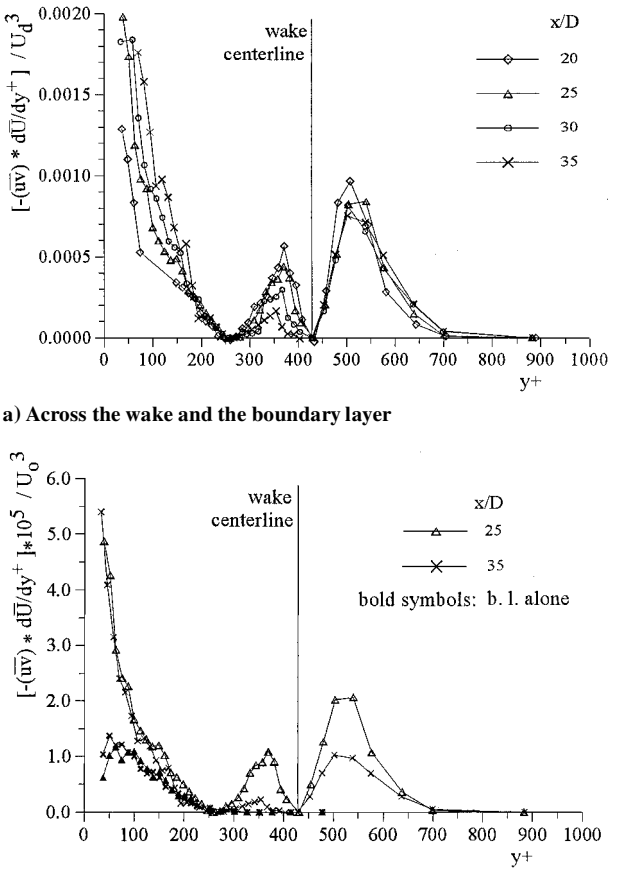

Fig. 4 Turbulent kinetic energy production.

determined from the directly measured momentum flux $uv(y, t)$. The slope $(d\bar{U}/dy^+)$ was calculated from the mean velocity profile, using a central difference approximation method. Profiles of $-\overline{uv}(d\bar{U}/dy^+)$, normalized by the local maximum velocity defect in the wake U_d, are shown in Fig. 4a. Three distinct areas of intensive energy production exist, corresponding to the upper-half wake ($440 < y^+ < 750$), the lower-half wake ($270 < y^+ < 440$), and the boundary layer ($y^+ < 270$). In the upper-half wake there is no significant streamwise variation in energy production distribution. At every measuring station considered energy production peaks at a lateral distance of about one diameter from the cylinder (i.e., at $y^+ \approx 530$). This distance corresponds to the location of the saddle points in the coherent flowfield model proposed by Hussain and Hayakawa.[8] According to that model, saddle points are associated with maximum shear stress caused by vortex stretching and consequently, with intensive energy production. As noted in Fig. 4a, there is a gradual reduction of peak kinetic energy production in the streamwise direction. This is attributed to a reduction of the strength of the coherent vortices as they move downstream.

In the lower-half wake there is significant reduction of peak energy production with increasing values of x/D. It seems that at $x/D = 20$ and 25 the kinetic energy production distribution is the mirror image of that in the upper-half wake up to the peak value ($y^+ \approx 360$). After that, energy production reduces steeply to zero close to the undisturbed boundary-layer outer limits ($y^+ \approx 270$). That implies that the kinetic energy production mechanism in the lower-half wake (i.e., vortex stretching) has been weakened, which is in accordance with the comments based on Figs. 3a and 3b. It was mentioned there that the strength of the large-scale vortices in the lower-half wake reduces as they move downstream because of their interaction with the boundary layer. Figure 4a shows the drastic effect of this interaction process on the turbulent kinetic energy production.

A substantial and also very steep increase of kinetic energy production is observed close to the plate ($y^+ < 160$). For a more detailed investigation of that region, the turbulent kinetic energy production curves for $x/D = 25$, 35 have been plotted again in Fig. 4b, together with corresponding curves obtained with the cylinder removed from the flow. All curves in Fig. 4b have been normalized with the freestream velocity U_0 for compatibility. The effect of the presence of the wake is apparent. An overview of the kinetic energy production distribution in the present flow indicates an important interaction between the lower-half wake and the boundary layer.

Figures 5a and 5b show the distribution of the turbulent kinetic energy components across the wake and the boundary layer. As it can easily be observed, peak values of $\overline{u^2}$ in the wake are very little affected by the streamwise distance, but peak values of $\overline{v^2}$ decrease considerably as x/D increases. This effect is also shown in the distribution of the kinetic energy parameter $\overline{s^2}$ $(=\overline{u^2} + \overline{v^2})$, shown in Fig. 5c. The quantity $\overline{s^2}$ appears to be concentrated at the wake centerline region, although there is no production there (refer to Fig. 4a). This leads to the conclusion that the kinetic energy in that region originates from the cylinder's shear flow. The fact that it diminishes with streamwise distance supports this argument. Furthermore, the kinetic energy distribution curves become wider as x/D increases. This is attributed to the energy production, which takes place in each half of the wake, especially in the upper half.

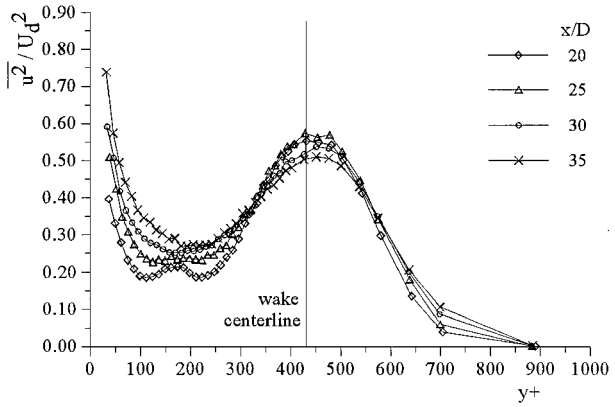

a) $\overline{u^2}$ component

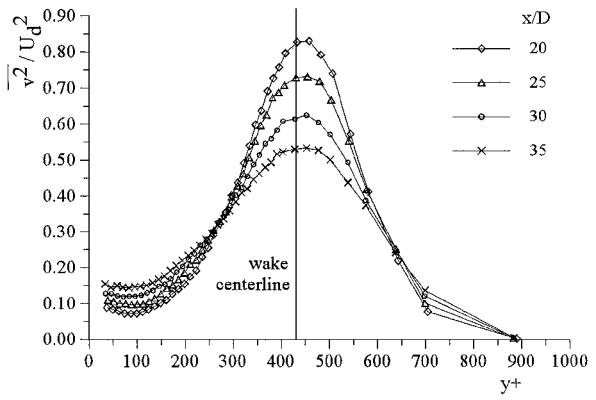

b) $\overline{v^2}$ component

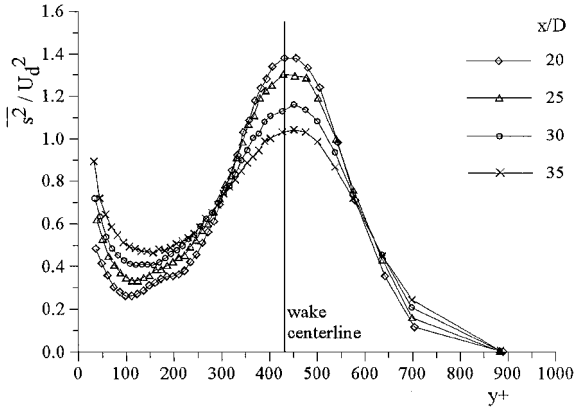

c) $\overline{s^2} = \overline{u^2} + \overline{v^2}$

Fig. 5 Turbulent kinetic energy distribution normal to the plate.

Although the peak values of $\overline{v^2}/U_d^2$ in the wake are in good agreement with the corresponding experimental values found in the literature,[20] peak values of $\overline{u^2}/U_d^2$ are about 30% higher. This is attributed to the surface roughness effect of the cylinder, which has been found also to have some connections to the two-dimensional character of the flow. The fact that the surface roughness of the cylinder affects preferably the streamwise velocity fluctuations may offer an explanation, in physical terms, of the enhancement of the two-dimensional character of the flow. Referring again to the coherent flowfield model of Hussain and Hayakawa,[8] the argument can be made that the enhanced streamwise small-scale fluctuations (dissipation) introduced to the wake by the cylinder's shear flow have an adverse effect on the streamwise vortical structures (the ribs, in Hussain and Hayakawa's terminology), which are located in between the transverse large-scale vortices (the rolls). A direct result of a reduction in the strength of the ribs is the weakening of the turbulence production mechanism (vorticity stretching) and, hence, the dominance of the rolls, which definitely have a quasi-two-dimensional character.

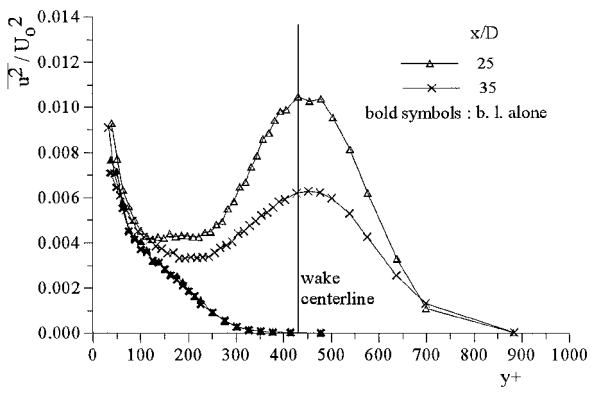

a) $\overline{u^2}$ component

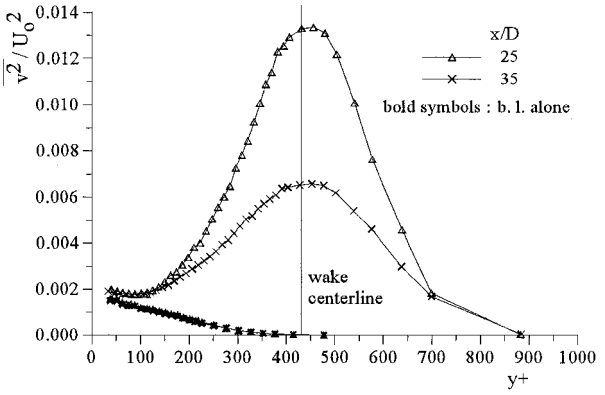

b) $\overline{v^2}$ component

Fig. 6 Effect of the wake on the kinetic energy distribution normal to the plate.

The effect of the presence of the wake on normal distribution of the kinetic energy components $\overline{u^2}$ and $\overline{v^2}$ is shown in Fig. 6. Figure 6a shows that the influence of the wake on the streamwise component is limited to $y^+ \approx 100$, whereas the influence to the normal component extends closer to the plate.

D. Turbulent Kinetic Energy Transport

The energy transport terms $\overline{u^3}$, $\overline{u^2v}$, $\overline{v^2u}$, $\overline{v^3}$, as well as $\overline{u^2s}$ and $\overline{v^2s}$, have been evaluated. Because, $\overline{u^2}$, $\overline{v^2}$, and $\overline{s^2}$ are always positive, the sign of the transport terms determine the sign of the associated velocity component and, hence, the direction of energy transport.

1. *Lateral Transport of the Kinetic Energy Components* $\overline{u^2}$, $\overline{v^2}$

Results for the more important lateral energy transport are shown in Figs. 7a and 7b. Both components of turbulent kinetic energy $\overline{u^2}$ and $\overline{v^2}$ are transported in the wake by the normal velocity fluctuations away from the centerline ($\overline{v^2u}$ and $\overline{v^3}$ are positive in the upper-half wake and negative in the lower-half wake). Considering the energy production distribution plot (Fig. 4a), one can easily deduce that turbulence transports kinetic energy away from the regions of intensive production. Although energy production in the lower-half wake has been drastically affected by the interaction with the boundary layer, turbulent energy transport in the lateral direction has only slightly been affected. The most significant difference between the distribution of the $\overline{v^2u}$ and $\overline{v^3}$ in the two halves of the wake is a more pronounced decline of peak values along the streamwise direction in the lower-half. Figures 8a and 8b indicate that the lateral transport of both kinetic energy components in the boundary-layer region is significant only in the presence of the wake.

2. *Streamwise Transport of the Kinetic Energy Components* $\overline{u^2}$, $\overline{v^2}$

The transport of the turbulent kinetic energy components $\overline{u^2}$ and $\overline{v^2}$ by the streamwise velocity fluctuations $u(t)$ is presented in Figs. 9a and 9b. Referring to Figs. 7a and 7b, the deduction can be made that streamwise transport of kinetic energy in the wake is

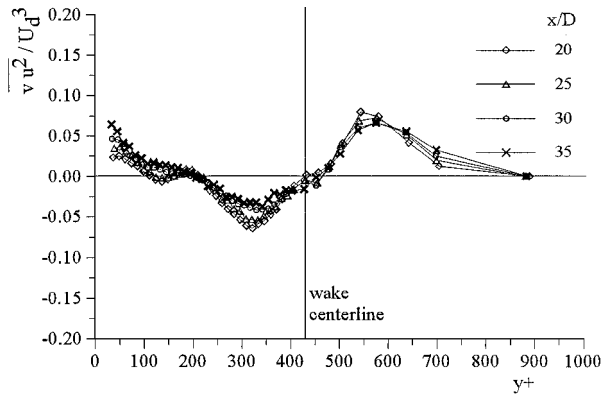

a) $\overline{u^2}$ component

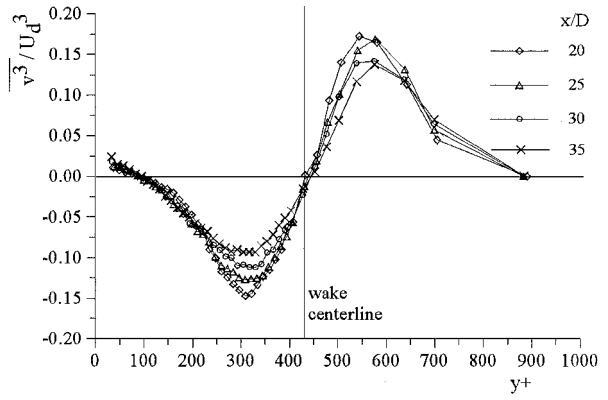

b) $\overline{v^2}$ component

Fig. 7 Lateral transport of the turbulent kinetic energy components.

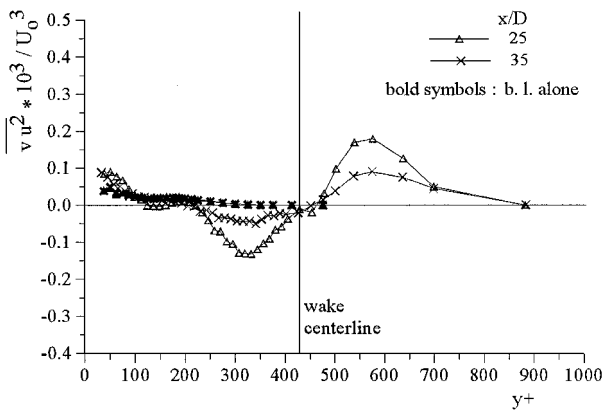

a) $\overline{u^2}$ component

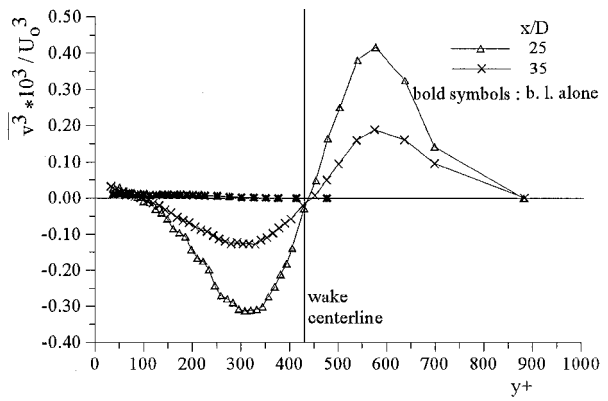

b) $\overline{v^2}$ component

Fig. 8 Effect of the wake on the lateral transport of the kinetic energy components.

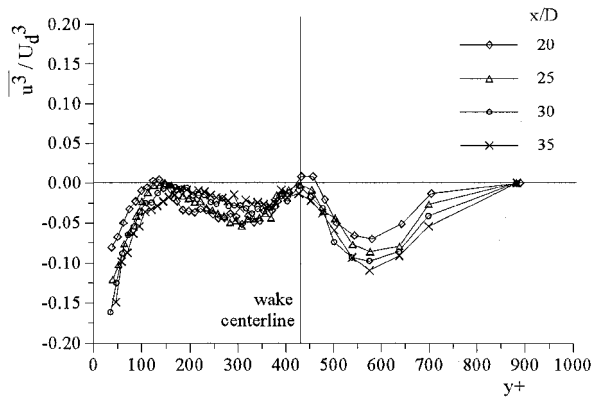

a) $\overline{u^2}$ component

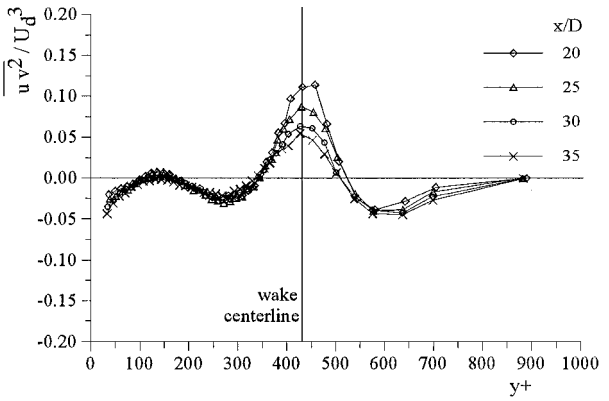

b) $\overline{v^2}$ component

Fig. 9 Streamwise transport of the turbulent kinetic energy components.

appreciably weaker compared to lateral transport. Figure 9a shows that there is strong upstream (relative to the local mean velocity) transport of the $\overline{u^2}$ component in the upper-half wake. The absolute peak values of $\overline{u^3}/U_d^3$ increase with streamwise distance. At the wake centerline $\overline{u^3}/U_d^3$ tends to zero, whereas in the lower-half wake it takes negative values again, but of much lower magnitude. Figure 9b shows clearly that the wake/boundary-layer interaction has very limited effect on the streamwise transport of $\overline{v^2}$. Strongest transport (in the streamwise direction) appears in the vicinity of the wake centerline. There are also two peaks of upstream transport of $\overline{v^2}$ at a distance of about $1.6D$ on either side of the centerline. Within the boundary layer the streamwise transport of $\overline{u^2}$ only has appreciable magnitude either with or without the presence of the wake (Figs. 10a and 10b).

3. Transport of $\overline{s^2} = \overline{u^2} + \overline{v^2}$

Figures 11a and 11b summarize the streamwise and lateral transport characteristics of turbulent kinetic energy, presented in Secs. III.D.1 and III.D.2. In the wake lateral transport is more intense than streamwise transport, whereas in the boundary layer the latter dominates. The wake/boundary-layer interaction process has a significant adverse effect on $\overline{u^2 s}$, whereas its effect on $\overline{v^2 s}$ becomes appreciable only at the larger x/D values. Lateral transport in both halves of the wake occurs in a direction away from the wake centerline. Streamwise transport changes sign at some point in each half wake. Close to the centerline, energy transport occurs in the downstream direction. In the outer region energy transport takes place in an upstream (relative to the mean flow) direction. Combining the information given in Figs. 11a and 4a, the deduction is made that the point of streamwise transport reversal is in the vicinity of maximum kinetic energy production.

Considering $\overline{u^2 s}$ and $\overline{v^2 s}$ at every point in the present flowfield as the magnitudes of the energy flux vectors along the horizontal and vertical directions respectively, turbulent kinetic energy transport is presented in Fig. 12 in vector form, according to the relation

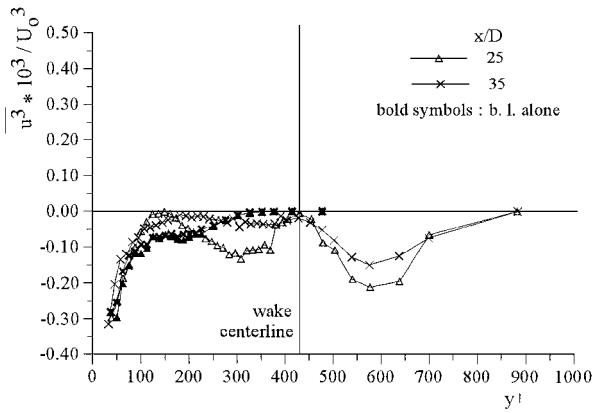

a) $\overline{u^2}$ component

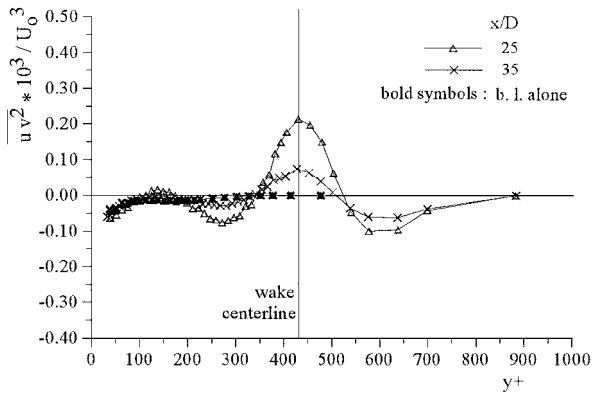

b) $\overline{v^2}$ component

Fig. 10 Effect of the wake on the streamwise transport of the kinetic energy components.

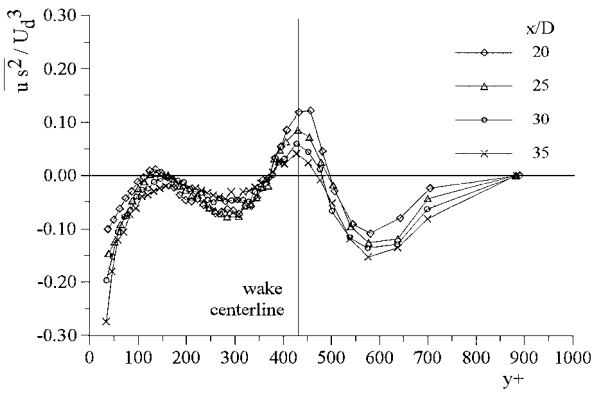

a) Streamwise

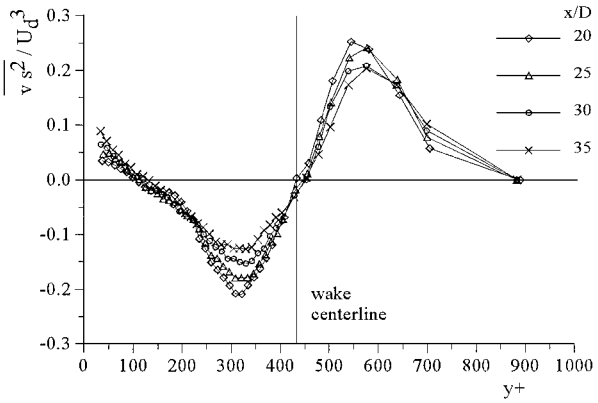

b) Lateral transport

Fig. 11 Turbulent kinetic energy parameter: $\overline{s^2}$ ($= \overline{u^2} + \overline{v^2}$).

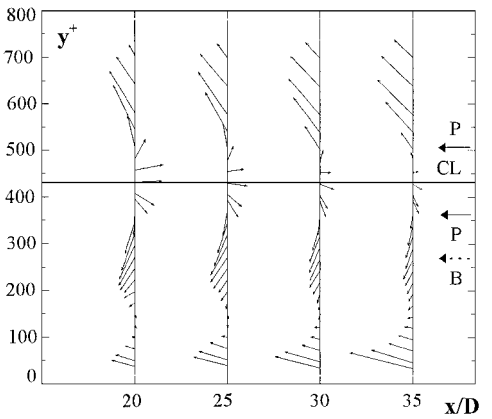

Fig. 12 Vector plot relative to the mean flow of the turbulent kinetic energy flux in the present flow. Flow direction, left to right; CL, wake centerline; P, points of peak energy production in the wake; and B, undisturbed boundary-layer thickness.

$$\boldsymbol{Q}_T = (\overline{u_s^2}/U_d^3)\boldsymbol{i} + (\overline{v_s^2}/U_d^3)\boldsymbol{j} \tag{1}$$

where $\boldsymbol{i}$ and $\boldsymbol{j}$ are unit vectors along the streamwise ($x-$) and normal (y^+-) directions, respectively. $\boldsymbol{Q}_T$ is thus the kinetic energy flux vector in the $x-y^+$ plane. $\overline{u^2 s}$ and $\overline{v^2 s}$ have been calculated using the velocity fluctuation components $u(t)$ and $v(t)$. Hence, energy flux vectors may appear in Fig. 12 pointing in the upstream direction (i.e., from right to left) because they are referenced to the local mean velocity. Close to the centerline, transport of the kinetic energy originating from the cylinder's shear flow diminishes rapidly as x/D increases. After the points of peak energy production caused by vortex stretching (Sec. III.C), locally produced kinetic energy is directed upstream (relative to the local mean flow). In the upper-half wake energy flux does not change significantly with x/D, either in magnitude or direction, presumably because of the significant local production. In the lower-half wake energy transport toward the boundary layer weakens progressively with streamwise distance because of the continuous reduction of local energy production. Well within the boundary layer, considerable energy flux occurs toward the wake because of the intensive energy production in that region.

IV. Conclusions

The experimental results of this work suggest that in the present complex flow with enhanced quasi-two-dimensional characteristics the large-scale flow organization in the cylinder wake has the dominant role in turbulent kinetic energy production and transport. Apart from the region close to the wake centerline, where the kinetic energy originates from the cylinder's shear layer, the intense energy production recorded in both halves of the wake is attributed to large-scale vortex stretching. The wake/boundary-layer interaction process has a significant adverse effect on the strength of the vortices and the kinetic energy production process in the lower-half wake, causing considerable reduction of turbulent kinetic energy production in that region. On the other hand, a large increase of kinetic energy production has been observed in the boundary-layer flow, as a result of the presence of the wake. Regarding energy transport, there is intensive transport toward the freestream in the upper-half wake, where the coherent vortices are least affected by the wake/boundary-layer interaction process at all streamwise locations considered. In the lower-half wake, however, energy flux toward the plate diminishes rapidly as streamwise distance increases. This is accompanied by a nearly constant flux of kinetic energy from the boundary layer toward the wake, indicating a significant exchange of kinetic energy between the two flows. As the wake/boundary-layer interaction develops, the energy exchange proceeds clearly in favor of that from the boundary layer.

Acknowledgment

The present work was supported by the European Communities Commission under Contract AVI-CT92-0017.

References

[1]Turner, J. J., "Turbulent Entrainment: The Development of the Entrainment Assumption and Its Application to Geophysical Flows," *Journal of Fluid Mechanics*, Vol. 173, Dec. 1986, pp. 431–471.

[2]Lin, S. J., and Corcos, G. M., "The Mixing Layer: Deterministic Models of a Turbulent Flow, Part 3. The Effect of Plane Strain on the Dynamics of Streamwise Vortices," *Journal of Fluid Mechanics*, Vol. 141, April 1984, pp. 139–178.

[3]Hussain, A. K. M. F., "Coherent Structures and Turbulence," *Journal of Fluid Mechanics*, Vol. 173, Dec. 1986, pp. 303–356.

[4]Browne, L. W. B., Antonia, R. A., and Shah, D. A., "Turbulent Energy Dissipation in a Wake," *Journal of Fluid Mechanics*, Vol. 179, June 1987, pp. 307–326.

[5]Fabris, G., "Third-Order Conditional Transport Correlations in the Two-Dimensional Turbulent Wake," *Physics of Fluids*, Vol. 26, No. 2, 1983, pp. 422–427

[6]Tritton, D. J., *Physical Fluid Dynamics*, Reinhold, New York, 1977, pp. 18–29.

[7]Kiya, M., and Matsumura, M., "Turbulence Structure in the Intermediate Wake of a Circular Cylinder," *Bulletin of the Japan Society of Mechanical Engineers*, Vol. 28, No. 245, 1985, pp. 2617–2624.

[8]Hussain, A. K. M. F., and Hayakawa, M., "Eduction of Large-Scale Organized Structures in a Turbulent Plane Wake," *Journal of Fluid Mechanics*, Vol. 180, July 1987, pp. 193–229.

[9]Bearman, D. W., and Zdravkovich, M. M., "Flow Around a Circular Cylinder Near a Plane Boundary," *Journal of Fluid Mechanics*, Vol. 89, Pt. 1, Nov. 1978, pp. 33–47.

[10]Suzuki, K., Suzuki, H., Kikkawa, V., and Kigawa, H., "Study on a Turbulent Boundary Layer Disturbed by a Cylinder—Effect of Cylinder Size and Position," *Turbulent Shear Flows 7*, edited by F. Durst, B. E. Launder, W. C. Reynolds, F. W. Schmidt, and J. H. Whitelaw, Vol. 7, Springer–Verlag, Berlin, 1991, pp. 119–135.

[11]de Souza, F., Delville, J., Lewalle, J., and Bonnet, J. P., "Large Scale Coherent Structures in a Turbulent Boundary Layer Interacting with a Cylinder Wake," *Experimental Thermal and Fluid Science Journal*, Vol. 19, No. 4, 1999, pp. 204–213.

[12]Doligalski, T. L., Smith, C. R., and Walker, D. A., "Vortex Interactions with Walls," *Annual Review of Fluid Mechanics*, Vol. 26, 1994, pp. 573–616.

[13]Chuang, F. S., and Conlisk, A. T., "The Effect of Interaction on the Boundary Layer Induced by a Convected Rectilinear Vortex," *Journal of Fluid Mechanics*, Vol. 200, March 1989, pp. 337–365.

[14]Luton, A., Ragab, S., and Telionis, D., "Interaction of Spanwise Vortices with a Boundary Layer," *Physics of Fluids*, Vol. 7, No. 11, 1995, pp. 2757–2765.

[15]Boer, G. J., and Sepherd, T. G., "Large-Scale, Two-Dimensional Turbulence in the Atmosphere," *Journal of Atmospheric Sciences*, Vol. 40, No. 1, 1983, pp. 165–184.

[16]Tennekes, H., "Turbulent Flow in Two and Three Dimensions," *Bulletin of the American Meteorological Society*, Vol. 59, No. 1, 1978, pp. 22–28.

[17]Sideridis, G. A., Kastrinakis, E. G., and Nychas, S. G., "Experimental Simulation of Air Pollution Dispersion by Atmospheric Motions," *Proceedings of the Air Pollution III Conference*, edited by H. Powel, N. Moussiopoulos, and C. A. Brebbia, Vol. 2, Computational Mechanics Publications, Boston, 1995, pp. 177–184.

[18]Hama, F. R., "An Efficient Tripping Device," *Journal of the Aeronautical Sciences*, Vol. 24, No. 3, 1957, pp. 236, 237.

[19]Jayesh, Tong, C., and Warhaft, Z., "On Temperature Spectra in Grid Turbulence," *Physics of Fluids*, Vol. 6, No. 1, 1994, pp. 306–312.

[20]Matsumura, M., and Antonia, R. A., "Momentum and Heat Transport in the Turbulent Intermediate Wake of a Circular Cylinder," *Journal of Fluid Mechanics*, Vol. 250, May 1993, pp. 651–668.

J. C. Hermanson
Associate Editor